Available online at www.sciencedirect.com
ScienceDirect
Biosensors and Bioelectronics 22 (2007) 2261–2267
BIOSENSORS & BIOELECTRONICS
www.elsevier.com/locate/bios

Amplification of fluorescence with packed beads to enhance the sensitivity of miniaturized detection in microfluidic chip☆

Kyeong-Sik Shin[a,c], Sung Woo Lee[a], Ki-Cheol Han[b], Sang Kyung Kim[a], Eun Kyung Yang[b], Jung Ho Park[c], Byeong-Kwon Ju[d], Ji Yoon Kang[a,*], Tae Song Kim[a]

[a] *Microsystem Research Center, Korea Institute of Science Technology, Seoul, Republic of Korea*
[b] *Biomedical Research Center, Korea Institute of Science Technology, Seoul, Republic of Korea*
[c] *Department of Electronics Engineering, Korea University, Seoul, Republic of Korea*
[d] *School of Electrical Engineering, Korea University, Seoul, Republic of Korea*

Received 26 April 2006; received in revised form 11 September 2006; accepted 9 November 2006
Available online 13 December 2006

Abstract

This paper reports the pre-concentration of C-reactive protein (CRP) antigen with packed beads in a microfluidic chamber to enhance the sensitivity of the miniaturized fluorescence detection system for portable point-of-care testing devices. Although integrated optical systems in microfluidic chips have been demonstrated by many groups to replace bulky optical systems, the problem of low sensitivity is a hurdle for on-site clinical applications. Hence we integrated the pre-concentration module with miniaturized detection in microfluidic chips (MDMC) to improve analytical sensitivity. Cheap silicon-based photodiodes with optical filter were packaged in PDMS microfluidic chips and beads were packed by a frit structure for pre-concentration. The beads were coated with CRP antibodies to capture antigens and the concentrated antigens were eluted by an acid buffer. The pre-concentration amplified the fluorescence intensity by about 20-fold and the fluorescence signal was linearly proportional to the concentration of antigens. Then the CRP antigen was analyzed by competitive immunoassay with an MDMC. The experimental result demonstrated that the analytical sensitivity was enhanced up to 1.4 nM owing to the higher signal-to-noise ratio. The amplification of fluorescence by pre-concentration of bead-based immunoassay is expected to be one of the methods for portable fluorescence detection system.

Keywords: Pre-concentration; Beads; Immunoassay; Fluorescence detection; Photodiode

1. Introduction

Point-of-care testing is one of the most promising applications of lab on a chip owning to the portability of diagnostic chips and small reagent consumption. The miniaturization, system integration, and parallelization of microfluidic systems afford many performance enhancements in terms of speed, analytical efficiency and throughput. For example, the long capillary or bead column for biochemical reactions has been miniaturized into one chip, thereby reducing the size of analytical equipment down to palm-top size. However, fluorescence detection systems are still bulky and unsuitable for portable applications due to the large volume and high equipment cost such as fluorescence microscope with PMT or cooled CCD. In addition, the small volume and the short optical path of the microfluidic channel make fluoresce detection of biomolecules more difficult (Mogensen et al., 2004).

Many research groups have been studying the integration of optical detection systems to reduce detection system size with optical fiber or small photodetectors. PMT was integrated in microfluidic channels (Johnson and Landers, 2004; Namasivayam et al., 2004) and optical fiber was inserted in PDMS microchips to transmit the external laser source for compact substitution of the Laser Induced Fluorescence (LIF) detector (Li et al., 2004). Although PMT is capable of single-photon response, the integration of PMT has limitations in portable diagnostic systems since it is relatively larger and much more expensive. Hence, silicon-based photodiodes are a good substitute for PMT because of their easy integration with microfluidic chips, and low cost due to the well-established fab-

☆ This paper was presented at Biosensors 2006 and is being submitted to the special issue of biosensors and bioelelctronics devoted to Biosensors 2006.

* Corresponding author at: Microsystem Research Center, Korea Institute of Science Technology, 136-791 Seoul, Republic of Korea. Tel.: +82 2 958 6747.
E-mail address: jykang@kist.re.kr (J.Y. Kang).

0956-5663/$ – see front matter © 2006 Elsevier B.V. All rights reserved.
doi:10.1016/j.bios.2006.11.011

rication process in microfabrication foundries. Some research groups fabricated PIN photodiodes as a photodetector on silicon or glass substrates to bypass the excitation light (Chabinyc et al., 2001; Jorgensen et al., 2003; Kamei et al., 2003) and others developed complex optical schemes such as waveguide, optical fiber or microlens (Epstein and Walt, 2003; Jang et al., 2005; Roulet et al., 2001). However, the simplest and most inexpensive configuration of the suggested methods is a fully packaged photodiode covered with an interference filter (Chabinyc et al., 2001; Jorgensen et al., 2003; Shin et al., 2006b), if the problems of packaging and low sensitivity can be solved. We have suggested PDMS (polydimethylsiloxane) packaging for the photodiode and analyzed the analytical sensitivity in a simple microfluidic channel (Shin et al., 2006a).

Despite the efforts to integrate the miniaturized fluorescence detection system in microfluidic chips, the limit of detection (LOD) is still higher than that of the external detection system due to the intrinsically low sensitivity of the photodetector. Therefore, amplification of the fluorescence signal is important to overcome the low performance of the integrated detection system. Since the microfluidic chip can combine several processes in a chip, the integration of pre-concentration is a nice candidate for the improvement of the fluorescence signal. Although enhancing the fluorescence signal can be achieved by the higher quantum efficiency of fluorophor, material selection is usually limited to available commercial products. On-chip sample pre-treatment is possible with various techniques such as FAS (field-amplified sample stacking), FAI (filed-amplified injection), ITP (isotachphoresis), and SPE (solid-phase extraction) (Lichtenberg et al., 2003; Razpotnik et al., 2003). FAS, FAI and ITP can be implemented in electrokinetically driven systems with a high voltage sequencer; however they are not applicable for pressure driven microfluidic systems. SPE is the process with which the analyte is captured at an appropriate stationary phase and subsequently eluted in concentrated form. Selective extraction and pre-concentration of antigens can be processed by reaction of the antibody-coated beads. Antigens with high affinity for the antibodies are retained on the beads, while other biomolecules are washed away. Then the eluted SPE solution is exploited in heterogeneous immunoassay. The concentration efficiency of SPE is in the range of 80–500 (Montpetit et al., 2005; Razpotnik et al., 2003; Oleschuk et al., 2000), which is higher than other methods by about 5- to 10-folds. Especially, Oleschuk et al., reported that concentration efficiency was enhanced up to 500 times with a chamber using two weirs. Hence bead-based heterogeneous immunoassay with SPE can enhance the LOD of integrated detection systems by at least one order. Therefore, we integrated pre-concentration modules to compensate for the low photodiode sensitivity and investigated the enhancement of the fluorescence signal.

In this article, we report the fluorescence detection of a disease marker, CRP (C-reactive protein) antigen, using a pre-concentration and integrated photodiode. CRP was selected since it is widely used as a target marker for the performance test of developed biosensors (Hu et al., 2006; Kartalov et al., 2006; Lee et al., 2005). The fundamental characteristics of bead-based concentration were studied by external PMT and the CRP antigen was analyzed by competitive immunoassay. The fluorescence of eluted CRP antigen was detected by the photodiode after analyte antigens competitively bound to the antibody on stationary beads. Based on the experimental results, the feasibility of the pre-concentrated bead immunoassay with miniaturized fluorescence detection in microfluidic chips (MDMC) is discussed in terms of assay performance such as LOD and reliability.

2. Material and methods

2.1. Reagents

All reagents were of analytical grade and the solutions were purchased from Sigma Aldrich (St. Louis, MO, USA). They were prepared with distilled water, which was boiled prior to preparation of the entire set of standards and reagents to make it free of dissolved oxygen. The blocking solution of the bead chip was a mixture of 5% bovine serum albumin (BSA, Sigma) in 137 mM sodium phosphate buffered saline (PBS, Sigma) of pH 7.4. Also, PBS was used as a basic buffer solution and a washing solution for bead chip. The polystyrene beads (goat anti-mouse IgG polystyrene, 15.18 μm diameter) and CRP antibody and antigen were purchased from Spherotech, IL, USA and Fitzgerald, MA, USA, respectively.

2.2. Photodiode design and fabrication

The PIN photodiode was fabricated on a silicon substrate and covered with an interference optical filter that was directly deposited on the substrate to enable the transmission of emitted fluorescence as well as blockage of background noise from the excitation light. A PIN circular-type photodiode was designed for a lateral and shallow depletion region, improving the collection efficiency. It was reported that the most visual spectrum range is absorbed within 1 μm depth of the silicon from the oxide interface (Chamberlain, 1979; Kyomasu, 1995). Therefore, we designed a junction depth of 150 nm in the p^+ region. The circular-type photodiode with a diameter of 350 μm was adopted to collect the dispersed light considering the distance from the fluidic channel of the bead chip to the photodiode. The fabrication process of the designed photodiode was simulated by TSupreme^{TM} and the depth at the maximum concentration in the p^+ region was calculated to be 80 nm thick.

The PIN photodiode was fabricated on an n-type silicon substrate with a resistivity of 4 kΩ cm. Arsenic was implanted by an energy level of 80 keV and a dose of $3 \times 10^{15}\,cm^{-2}$ to form the n^+ and p^+ regions, and boron was implanted by an energy level of 30 keV and a dose of $5 \times 10^{15}\,cm^{-2}$. After implantation, the annealing step was carried out to activate the dopants. TEOS (tetraethooxysihme) silicon dioxide was deposited as a passivation layer of 500 nm thickness. An optical inference filter of 2.3 μm thickness was directly deposited on the photodiode, which consists of 16 pairs of SiO_2/TiO_2 layers. Finally, for the metal connection, contact holes were patterned, and aluminum electrodes were formed by a metallization process.

2.3. Design of microfluidic chip for bead immunoassay

Since the chip was driven by vacuum pressure, we needed to estimate the pressure drop across the chamber to ensure chip operation. The pressure across the bead chamber was calculated by Ergun's equation:

$$\frac{\Delta P}{L} = 150\frac{\mu Q}{D_p^2 wh}\frac{(1-\varepsilon)^2}{\varepsilon^3} \quad (1)$$

where Q, and ΔP are the flow rate and pressure drop. L, w, and h are the length, width and depth, respectively, of the packed bead chamber. ε, μ and D_p are the void fraction of packing, fluid viscosity and bead diameter, respectively. If we assume the packing structure is face-centered cubic (FCC), the void fraction is about 0.26. When the driving vacuum pressure is 5 psi, the flow rate is 3 μL/min and the flow speed is 2 mm/s. The flow resistance of the channel is less than 10% of total resistance. The volume of the chamber is 24 nL and the liquid volume of the chamber is 6.24 nL. The binding capacity of the bead is 0.15 μg/mg and the number of beads is 9.7×10^3, considering the volume of the chamber. When all antibodies coated on the beads bind to the antigen, the theoretical maximum concentration can increase up to 453 μg/mL. When the velocity is 2 mm/s and the flow rate is 60 nL/s, the duration of the eluted peaks is 0.2 s, if we assume antigen detachment occurs instantaneously. However, the elution peak was broadened due to the chemical reaction and the condition of the bead-packing.

2.4. Microfluidic chip fabrication and photodiode packaging

The PDMS microfluidic chip was fabricated by soft lithography with silicon mold etched by deep reactive ion etching. The channel pattern is presented in Fig. 1, where the exploded view shows the part of the bead injection and the frit structure. The width, length and depth of the chamber were 1 mm × 0.8 mm × 30 μm and the size of the frit was 20 μm × 50 μm. The space between frits was 10 μm since the bead diameter was 15.17 μm. The lengths of the inlet channels from reservoirs 1, 2 and 3 to the junction were 3, 6 and 6 mm, respectively. The channel from the junction to the entrance of the bead chamber was 40 mm long and was curved to extend along the channel length for sufficient mixing of the target antigen and the standard fluorescence antigen. The length from the bead chamber outlet to the detection point was 8.5 mm. The widths and depths of all channels were 100 and 30 μm, respectively.

The microfluidic chip consists of PDMS (polydimethylsiloxane) and cover glass. PDMS and 150 μm-thick cover glass were used as a microfluidic channel layer and a bottom substrate in

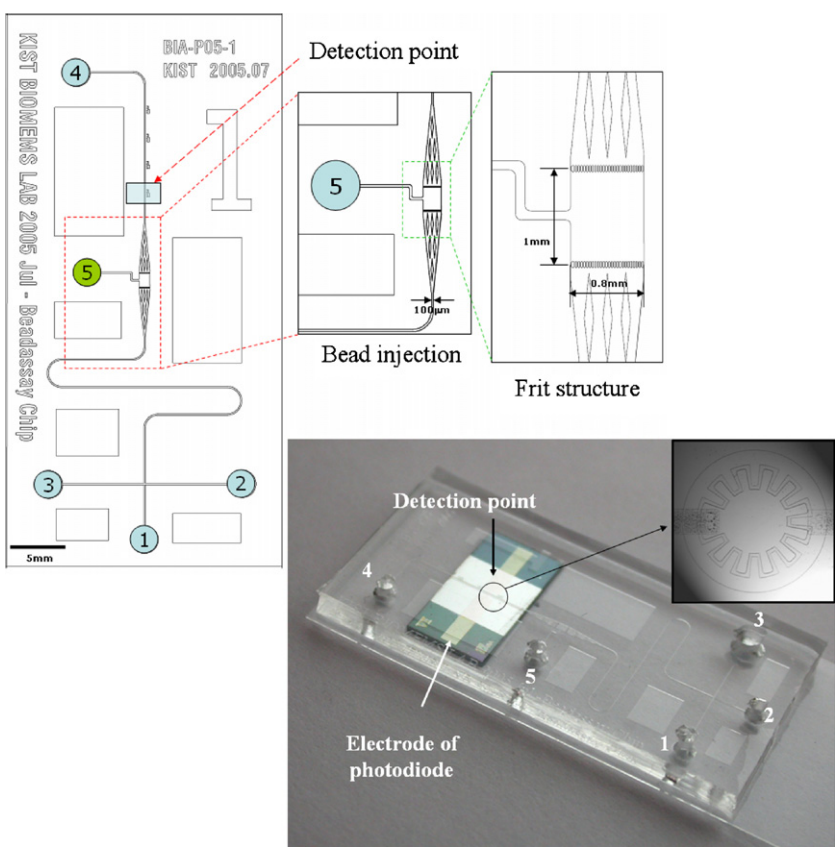

Fig. 1. Bead chip design and illustration. Schematic bead chip diagram (top). The width, length and depth of chamber are 1 mm × 0.8 mm × 30 μm and the size of the frit is 20 μm × 50 μm. The spaces between the frits are 10 μm and the lengths of the inlet channels from reservoirs 1, 2 and 3 to the junction are 3, 6 and 6 mm, respectively. The photograph of the bead chip (bottom), inset box, represents an embedded photodiode.

the bead chip, respectively. These two parts were bonded to form the bead chip slab with the process of oxygen plasma bonding (Lin et al., 2001; Satyanarayana et al., 2005).

To bond the photodiode with the bead chip slab, the packaging of the photodiode in PDMS was processed. The PDMS was spin-coated on the PES (polyether sulfone) flexible substrate to form a 20 μm-thick film (the gap from the cover glass to photodiode) followed by baking at 85 °C for 5 min. The photodiode was placed on the PDMS film face down and then liquid PDMS was poured on it to embed the photodiode in the PDMS slab. The PDMS was cured at room temperature overnight to avoid mechanical stress to the photodiode. This procedure allowed the liquid PDMS to flow under the wire connected to the metal electrode. The photodiode-embedded PDMS slab was removed with ease from the flexible PES substrate by a peeling-off process (Shin et al., 2006a). We bonded the cover glass of the bead chip slab with the PDMS slab through oxygen plasma bonding. The bottom of Fig. 1 illustrates the bead immunoassay chip with an integrated photodiode in MDMC. The total distance from the fluidic channel of the bead chip to the photodiode was about 170 μm. The photograph of the photodiode fabricated with a diameter of 350 μm is shown in the inset box of Fig. 1.

2.5. Preparation of beads and measurement system

The non-specific binding on polystyrene beads was blocked by 5% BSA in PBS. The beads in the tube (Eppendorf) were incubated with a BSA solution on the rocker at room temperature (RT) for 30 min, and were spun down at 3000 rpm for 5 min, followed by removal of the supernatant. The primary CRP antibody was added to the bead suspension and incubated in PBS on the rocker at RT for 1 h. The beads were collected by the previously described spin-down method, and washed by PBS on the rocker at RT for 15 min. Finally, the collected beads were diluted with a small amount of PBS (approximately 50 μL PBS in case of 100 μL beads).

To prevent absorption of the fluorescent dye in the channel, the surface of the channel was treated with 5% BSA in PBS at RT in a vacuum chamber to remove bubbles trapped inside the channel. In order to pack the beads into the chip chamber, the beads were loaded in inlet reservoir 5 while negative pressure was applied at the waste outlet (−2 psi or more if necessary). Then, three inlet reservoirs (1, 2 and 3) for the reagent were sealed by a cover glass. After the beads were thoroughly packed in both the chamber and the bead-supplying channel, epoxy was added in inlet reservoir 5 and cured for about 20 min to fix the packed beads.

After removing the cover glass on the inlet reservoirs, the fluorescein-labeled and unlabeled-CRP antigen mixture was loaded in inlet reservoir 1 and negative pressure (typically −5 psi) was applied at the waste outlet. After binding the fluorescein-labeled CRP antigens to the antibodies, the non-specifically bound species were washed away with a PBS solution. Finally, the elution buffer of 0.1 M glycine (pH 1.8) was passed through the chamber to elute the fluorescein-labeled CRP antigen which was bound to the antibody-coated beads. The fluorescence signal was monitored simultaneously by an external PMT and an integrated photodiode in the MDMC at the detection point in the microfluidic channel as indicated in Fig. 1. The photodiode current was recorded by a source and measurement system (Keithley 2601) and the emitted fluorescence in the channel was also recorded by PMT through a fluorescence microscope. A mercury lamp (Philips, 100 W) was the light source in the fluorescence detection and incidental light was filtered by an optical filter set (wavelength ∼ 488 nm). All instruments were run by a personal computer and data were collected by operating software.

3. Results and discussion

3.1. Specific binding of antigen, bead-packing and elution in bead chamber

The purchased beads had been coated by a secondary antibody against mouse IgG to bind the anti-CRP antibody (CRP-Ab). Non-specific binding was blocked by BSA coating and the fluorescein-labeled CRP antigen (CRP-Ag*) must therefore have reacted only with CRP-Ab. Neither the bead surface nor the secondary antibody should have reacted with CRP-Ag*. The binding of CRP-Ag* was clearly observed by the fluorescence on the beads after the Ab–Ag interaction. As a control experiment, CRP-Ag* was incubated with the secondary antibody-coated beads blocked by BSA. When the CRP-Ag* was incubated in suspension of the beads, fluorescence was not observed, which confirmed that the BSA blocking prevented CRP-Ag* from interacting with the beads. Specific binding of CRP-Ag* to CRP-Ab ensures that fluorescence detection of the beads can be analyzed the concentration of CRP-Ag* by bead-based immunoassay. The beads were packed into the chamber by the negative pressure applied on the outlet reservoir. Fig. 2A confirmed that the beads did not sneak out from chamber and were well packed in the chamber.

The elution procedure was first tested with the beads with which Ag* had been already bound since it is a critical process in bead-based assay. The CRP-Ag* of 5 μg/mL reacted with the CRP-Ab-coated beads in the tube on the rocker at RT, and the non-specific CRP-Ag* was washed away by PBS. After the beads were packed in the chamber, the elution buffer was injected into the chamber. The fluorescence intensity of the chamber was observed and the eluted signal was monitored with PMT at the detection point. The photographs of the fluorescence in chamber in Fig. 2B show that the antigens were eluted by glycine buffer. In the bottom image, we can observe residual antigens remaining in chamber by physical adsorption; however, we believe it could not have affected the peak magnitude of the eluted signal significantly even though it could have raised the baseline of the signal after elution. Fig. 2B shows the amplified fluorescence intensity of the eluted antigens when compared with non-concentrated antigens of 5 μg/mL. The amplification factor was 25-fold when the signal was integrated during the period of the full-width half-maximum (FWHM) of an eluted peak. However, the measured elution time is longer than that of the theoretical time since the concentration and pH of elution buffer could affect the elution time (Oleschuk et al., 2000). To

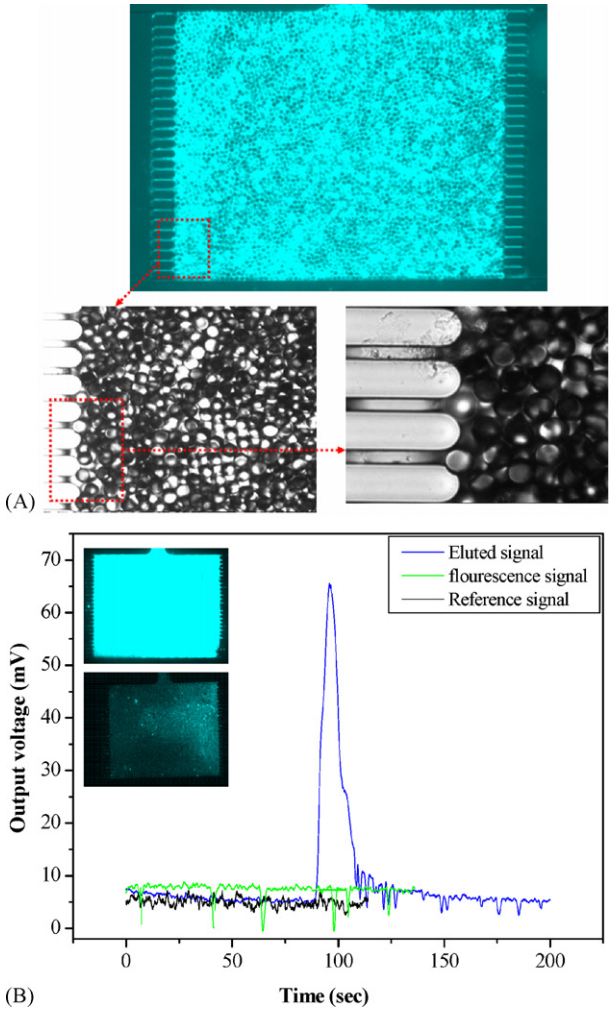

Fig. 2. Illustration of bead chamber. (A) Fully packed beads in chamber. (B) Graph of output signal at detection point during elution procedure; the inset box represents the fluorescence change in chamber during elution procedure (0 s, 40 s).

increase the amplification factor, we need to optimize the elution buffer to minimize the elution time since a longer elution time will decrease the amplification ratio.

3.2. Optical filter and detector performance

The interference filter deposited on the photodiode was used to filter out the excitation light from the fluorescence light. The fluorescein has its maximum absorption wavelength at 488 nm and maximum emission at 530 nm. Hence, the filter was fabricated to block more than 99.95% of the excitation light and to transmit more than 80% of the fluorescence within the range of 510–550 nm (inset box of Fig. 3). Filter efficiency is critical to sensor sensitivity because the background noise is largely dependent on the transmitted excitation light. Since the transmittance of 0.05% of incidental light is relatively larger than in the commercial LIF system, we needed to investigate the LOD of the photodetector with the filter. After the PDMS microfluidic channel with a dimension of 100 μm × 30 μm was filled with fluorescein, the photodiode current was measured with a mercury lamp as an excitation light. The concentration of fluorescein was varied from 500 nM to 2.5 μM. The background signal was as large as 397 nA with a deviation of 0.97 nA. The slope of the linear response was 94 nA/μM, as shown in Fig. 3. The LOD in the MDMC was at least 30 nM when the signal-to-noise ratio (SNR) was above 3.

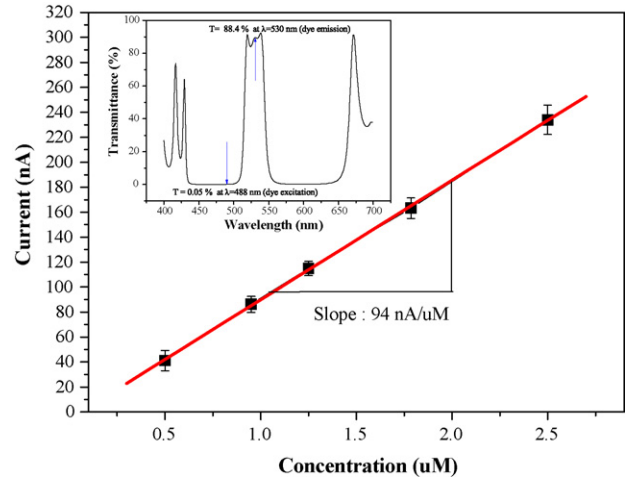

Fig. 3. Output currents of the photodiode with deposited interference optical filter as a function of fluorescein concentration; the inset box show the optical filter characteristics (transmittance as wavelength function in deposited interference optical filter on the photodiode. The filter was fabricated to block more than 99.95% of the excitation wavelength and transmit more than 80% of the fluorescence in the range of 510–550 nm).

3.3. Reaction of labeled CRP antigen and CRP antibody coated on the beads

To investigate the saturation time of the reaction of CRP-Ag* and CRP-Ab, the fluorescence intensity of the bead chamber was monitored by a PMT while the CRP-Ag* solution was injected into the bead chamber. As for the CRP-Ag* of 50 μg/mL, the fluorescence intensity curve was saturated in a few seconds, while the saturation of low concentration (e.g. 0.5 μg/mL) took too long to observe due to the bleaching of fluorescein. The calculated saturation time was about 1 h for the CRP-Ag* of 0.5 μg/mL, when the flow speed was assumed as 2 mm/s. It was difficult to record the fluorescence intensity for more than 10 min because the bleaching significantly deteriorated the signal. Therefore, we recorded the fluorescence of the bead chamber with CRP-Ag* of 5 μg/mL. The saturation time was 376 s, which was consistent with the calculated saturation time of 6 min. During the Ab–Ag reaction, the fluorescence intensity linearly increased with time, meaning that the binding number of CRP-Ag* linearly increased with the volume of the injected antigen solution. After equilibrium of the immuno-reaction was reached, the unbound antigen was washed out to prevent non-specific binding. PBS flushed out the non-specifically bound species in the chamber, and then the elution buffer was introduced into the chamber. The typical signal of the PMT during the washing and the elution of the chamber is shown in Fig. 4A. The first peak at 250 s describes the washing of the remained CRP-Ag* in the chamber and the PBS was stopped at 1300 s. When the elution

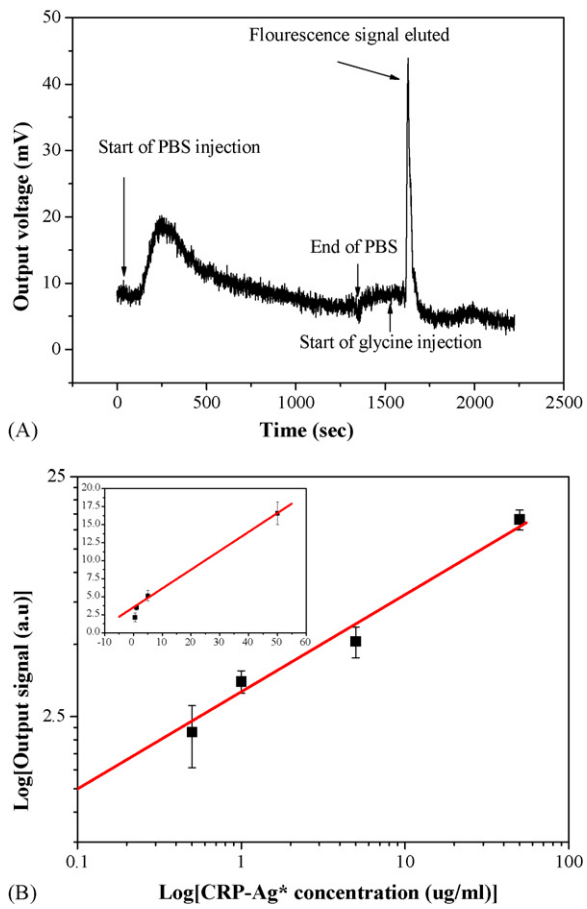

Fig. 4. Graphs of output signal and illustrations of elution procedure: (A) typical output signal of PMT during washing and elution of chamber procedure and (B) output signal as function of CRP-Ag* concentration with log–log scale and linear–linear scale in inset box, and photographs.

buffer was injected, the concentrated fluorescence peaked within 40 s.

CRP-Ag* was logarithmically diluted in PBS at the concentrations of 50, 5, 1, and 0.5 μg/mL and the reaction times of CRP-Ag* were 1 min, 10 min, 30 min, and 1 h, respectively. The eluted fluorescence intensity was measured with a PMT. The signal was analyzed through the integration of the calibrated values considering the background base signal (Fig. 4B). The graph shows the linearity of the integrated fluorescence to the concentration of CRP-Ag* and the pre-concentrated fluorescence can be used as an assay method. The experimental data was changed within the range of 7–11% except in the case of the lowest concentration. The fluorescence intensities at 0.5 μg/mL varied from the fitted line with an error of 21%, which was twice as large as those of the other points due to insufficient incubation time for the saturation of reaction. When the concentration of CRP-Ag* was low, the variation in bead-packing conditions and the flow speed might cause a large effect on the reaction time. Nevertheless, the experiment indicates the bead-packing and antigen binding was stable within a reasonable range except at the lowest concentration. If a more precise assay is necessary, the variation in the output signal can be reduced by optimizing the bead chamber and bead size.

3.4. Competitive immunoassay with bead chip

The immunoassay chip with an MDMC was used for the competitive immunoassay of the CRP antigen. The concentration of standard CRP-Ag* was fixed at 2.5 μg/mL and the concentration of CRP-Ag varied from 0 to 8 μg/mL in the mixture volume as shown in Table 1. When the mixture of CRP-Ag* and CRP-Ag flowed through the chamber, they reacted with CRP-Ab bound on the stationary beads. The fluorescence intensity in the bead chamber was proportional to the binding ratio of CRP-Ag* to CRP-Ab. As the concentration of CRP-Ag increased, the binding events of CRP-Ag* to the beads decreased and consequently the fluorescence intensity was reduced in the bead chamber. Thus, the CRP-Ag concentration of an unknown sample can be identified by the reduction of fluorescence.

The fluorescence intensity was measured by both a PMT and an integrated photodiode in the MDMC to crosscheck the output signals. Fig. 5A shows the results of competitive immunoassay of CRP-Ag with a PMT and an integrated photodiode. The graph shows a linear relationship between the concentration and the output signal of a photodiode in the MDMC. The signal of a photodiode was remarkably amplified when the analyte was concentrated by packed beads. Also, the signal of the photodiode was in good agreement with that of the PMT. To evaluate the LOD of the competitive assay, we plotted the fluorescence change as a function of the concentration of the non-labeled antigen, as seen in Fig. 5B. Immunoassay signal is the difference between the reference signal of CRP-Ag* without CRP-Ag and the measured signal with CRP-Ag added. The slope of the photodiode in the bead chip increased by about 20-fold after it was concentrated, as represented by *B*/*A* in Fig. 5B. This value is consistent with the result of a PMT measurement in Section 3.1, which represents the great increase in MDMC photodiode from 0.094 to 2.11 μA/μM due to the concentration. The increase of the output level in the photodiode provides more room to improve the LOD in fluorescence detection because the fluctuation of background noise is negligible due to the high signal to noise ratio. Considering that the fluctuation in the background signal was 0.97 nA (the value of which only changes by excita-

Table 1
Sample condition in competitive assay

	CRP-Ag*	CRP-Ag	Conversed fluorescence concentration	Binding time (min)
Concentration (μg/mL) in PBS (20 μL)	5	0, 4, 10, 8 (18)		
Concentration (μg/mL) in mixture (40 μL)	2.5	0, 2, 5, 8 (10)	2.5, 1.39, 0.83, 0.59 (0.5)	20
Concentration (nM) in mixture (40 μL)	120	0, 95, 240, 381 (476)	120, 66, 39, 28 (24)	20

() represents additional points in Fig. 5B.

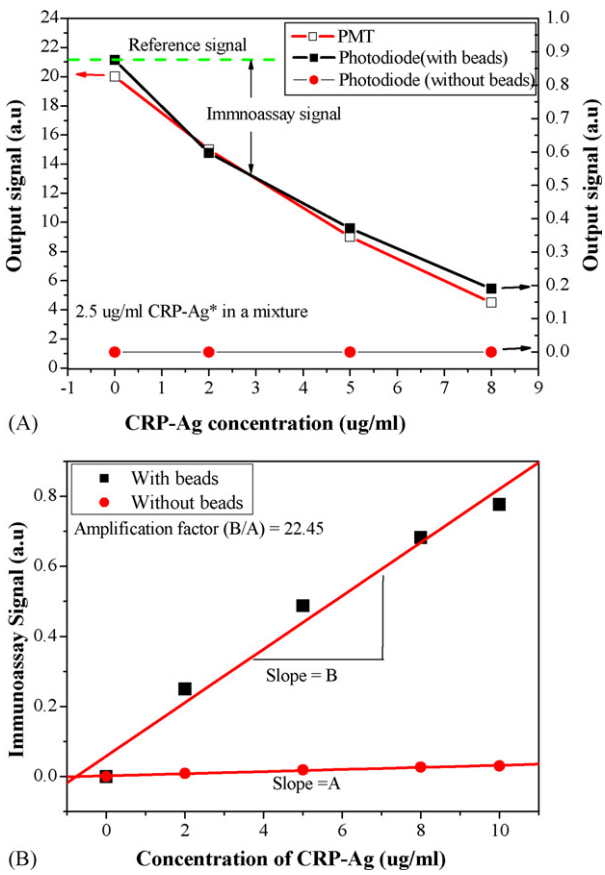

Fig. 5. Results of immunoassay. (A) Results of competitive CRP-Ag* and CRP-Ag immunoassay with PMT and photodiode. (B) Reduction in fluorescence intensity (which corresponded as immunoassay signal) as function of CRP-Ag concentration.

tion light intensity), the theoretical LOD could be estimated as 1.4 nM, an improvement of about 20 times.

To evaluate the LOD level at low concentrations, CRP-Ag* of 2.5 μg/mL as a standard concentration must be reduced to a level less than 0.25 μg/mL. However, we could not perform the lower concentration of CRP-Ag* as a standard in the competitive assay since the binding time dramatically increased as the concentration was lowered. Therefore, chip design improvement and the use of control fluorescence signals to minimize the error range in low concentrations can lower the LOD in future experiments.

4. Conclusions

We reported the competitive immunoassay of pre-concentrated CRP antigen by fluorescence detection using embedded photodiodes in microfluidic chips. A miniaturized fluorescence detection system was realized by the silicon-based PIN photodiode packaged in PDMS chip, and by the amplification of fluorescence signals with packed beads in a microfluidic chamber. We showed that the analytical sensitivity of the detection system was improved 20-fold by the enhanced signal-to-noise ratio and these pre-concentrations could compensate for low photodiode sensitivity. The portable detection of CRP-Ag could be possible in microfluidic chips with optimization of the bead-packing chamber and the elution buffer. Furthermore, the precise control of flow using electroosmosis is one of the ways to improve the LOD in portable detection devices.

Acknowledgement

This work was supported by the Intelligent Microsystem Center, which carries out one of the 21st century's Frontier R&D Projects sponsored by the Korea Ministry of Commerce, Industry and Energy.

References

Chabinyc, M.L., Chiu, D.T., McDonald, J.C., Stroock, A.D., Christian, J.F., Karger, A.M., Whitesides, G.M., 2001. Anal. Chem. 73, 4491–4498.
Chamberlain, S., 1979. IEEE Trans. Electron Devices 34, 7228–7231.
Epstein, J.R., Walt, D.R., 2003. Chem. Soc. Rev. 32, 203–214.
Hu, W.P., Hsu, H.-Y., Chiou, A., Tseng, K.Y., Lin, H.-Y., Chang, G.L., Chen, S.-J., 2006. Biosens. Bioelectron. 21, 1631–1637.
Jang, J.M., Shin, H.J., Hwang, S.W., Yang, E.G., Yoon, D.S., Kim, T.S., Kang, J.Y., 2005. Sens. Actuators B 108, 993–1000.
Johnson, M.E., Landers, J.P., 2004. Electrophoresis 25, 3513–3527.
Jorgensen, A.M., Mogensen, K.B., Kutter, J.P., Geschke, O., 2003. Sens. Actuators B 90, 15–21.
Kamei, T., Paegel, B.M., Scherer, J.R., Skelley, A.M., Street, R.A., Mathies, R.A., 2003. Anal. Chem. 75, 5300–5305.
Kartalov, E.P., Zhong, J.F., Scherer, A., Quake, S.R., Taylor, C.R., Anderson, W.F., 2006. Biotechniques 40, 85–90.
Kyomasu, M., 1995. IEEE Trans. Electron Devices 42, 1093–1099.
Lee, Y., Yoon, D., Kim, T., 2005. Integr. Ferroelectr. 69, 391–400.
Li, H.-F., Lin, J.-M., Su, R.-G., Uchiyama, K., Hobo, T., 2004. Electrophoresis 25, 1907–1915.
Lichtenberg, J., de Rooij, N.F., Verpoorte, E., 2003. Talanta 56, 233–266.
Lin, C.-H., Lee, G.-B., Lin, Y.-H., Chang, G.-L., 2001. J. Micromech. Microeng. 11, 726–732.
Mogensen, K.B., Klank, H., Kutter, J.P., 2004. Electrophoresis 25, 3498–3512.
Montpetit, S.A., Fitch, I.T., O'Donnell, P.T., 2005. J. Forensic. Sci., 50.
Namasivayam, V., Lin, R., Johnson, B., Brahmasandra, S., Razzacki, Z., Burke, D.T., Burns, M.A., 2004. J. Micromech. Microeng. 14, 81–90.
Oleschuk, R.D., Loranelle, L.S.-L., Yuebin, N., Har, D.J., 2000. Anal. Chem. 72, 585–590.
Razpotnik, P., Turšič, J., Veber, M., Novič, M., 2003. J. Chromatogr. A 991, 23–29.
Roulet, J.-C., Völkel, R., Herzig, H.P., Verpoorte, E., de Rooij, N.F., Dändliker, R., 2001. Opt. Eng. 40 (5), 814–821.
Satyanarayana, S., Karnik, R.N., Majumdar, A., 2005. J. Microelectromech. 14, 392–399.
Shin, K.-S., Kim, Y.-H., Min, J.-A., Kwak, S.-M., Kim, S.K., Yang, E.G., Park, J.-H., Ju, B.-K., Kim, T.-S., Kang, J.Y., 2006a. Anal. Chim. Acta 573/574, 164–171.
Shin, K.-S., Kim, Y.-H., Paek, K.-K., Jung-Ho, P., Eun-Gyeong, Y., Kim, T.-S., Kang, J.-Y., Ju, B.-K., 2006b. Electron Device Lett. IEEE 27 (9), 746–748.